Theoretical Survey of the Potential Energy Surfaces Associated with the $N^+(^3P,^1D) + C_2H_4$ Reactions in the Gas Phase†

Inés Corral, Otilia Mó, and Manuel Yáñez*

Departamento de Química, C-9, Universidad Autónoma de Madrid, Cantoblanco, 28049 Madrid, Spain

Received: April 22, 2004; In Final Form: May 21, 2004

The potential energy surfaces (PESs) associated with the reactions between ethylene and $N^+(^3P,^1D)$ ions have been investigated through the use of high-level G2(MP2) ab initio calculations. Although the $N^+(^3P) + C_2H_4$ entrance channel lies 46.7 kcal mol^{-1} below the $N^+(^1D) + C_2H_4$, most of the singlet-state cations are more stable than their triplet-state counterparts because, in general, the bonds in the former are stronger than those in the latter, favoring the crossover between both PESs. Several minimum energy crossing points between both hypersurfaces have been located, and the corresponding spin−orbit couplings indicate that spin-forbidden processes in $N^+ + C_2H_4$ reactions cannot be discarded. According to our survey, the product distribution in both $N^+(^3P) + C_2H_4$ and $N^+(^1D) + C_2H_4$ reactions should be quite different. While for the triplets the CNH^+, $HCNH^+$, $HCCH_2^+$, and $HCCH^+$ product ions should be observed, in agreement with the available experimental information, for the singlets the formation of CH_3^+ should be the dominant process.

Introduction

The chemistry of planetary atmospheres, cometary comae, and interstellar clouds is frequently governed by ion−molecule reactions. Such processes, normally including very simple molecular compounds, have received a great deal of attention, from both the experimental and theoretical points of view. It has been possible to obtain reliable rate constants in some cases and information about product distribution in many others.[1] However, in general much less is known about the possible mechanisms behind the reactions. Very often this information is obtained through the use of ab initio molecular orbital calculations[2−17] that, nowadays, have reached a level of accuracy that permits both confidence in the reliability of the potential energy surfaces (PESs) generated and identification of, in combination with spectroscopic techniques, interstellar species[9,18−21] elusive to experimental observation under normal laboratory conditions.

Particularly interesting are the reactions involving different small neutral compounds, such as water, ammonia, and formaldehyde, and singly charged atomic species that have relatively low lying excited states. This is the case of the halogen cations and N^+ where the first excited ^1D state is relatively close in energy to the ground ^3P state.[22] Quite importantly, however, when the ion is attached to a neutral molecule, a reverse stability order is often found and singlets become lower in energy than triplets,[8,13,23−28] reflecting the stronger bonds between the ion and the neutral in the former. Accordingly, different crossovers between singlet and triplet PESs can be envisaged,[13,26,28] and therefore in many of these processes spin-forbidden reaction mechanisms play an important role, as has been suggested before for $N^+ + SH_2$ and $N^+ + H_2CO$ reactions.[27,28] In this paper we will focus our attention on the reactions between $N^+(^3P,^1D)$ and ethylene, because hydrocarbons are ubiquitous in the aforementioned media and therefore they usually play an important role in the generation of new molecular systems.[29,30] As a matter of fact, ethylene is one of the main components of Titan's atmosphere,[29,31] where both $N^+(^3P)$ and $N^+(^1D)$ can be also produced from the existing N_2 molecules via cosmic ray absorption. Actually, in the laboratory both ionic species can be produced by electron impact dissociation of N_2 molecules.[32]

Although there is experimental information on the product distribution of the $N^+(^3P) + C_2H_4$ reaction,[33] the lack of theoretical information on this system is almost complete, and to the best of our knowledge the first paper dealing with some peculiarities of the $[C_2, H_4, N]^+$ singlet-state cations was published by us.[34] It must be mentioned that when the present work was about to be completed, a theoretical survey of the $[C_2H_4 + N^+]$ triplet potential energy surface was reported in the literature.[17] However, in this paper, the authors only consider the processes leading to hydrogen elimination, and no attention was paid to the possible coupling between triplet and singlet PESs.

Computational Details

The structures of the different stationary points of the $[H_4, C_2, N]^+$ singlet and triplet PESs have been obtained at the MP2-(f.c.)/6-31G(d) level of theory. The harmonic vibrational frequencies were obtained at the same level to characterize the different stationary points as local minima or transition states and to estimate the corresponding zero point vibrational energies (ZPE), which were scaled by the empirical factor 0.9646.[35] Final energies were obtained at the G2(MP2) level.[36] Hence, final energies are formally of a QCISD(T)/6-311+G(3df,2p) quality.

In those situations where some kind of instability appears, in particular symmetry-breaking problems, highly correlated methods as QCISD, CCSD, and CCSD(T) have been used for the geometry optimizations.

The crossover between both PESs was investigated by locating the most relevant minimum energy crossing points (MECPs) through the use of CASSCF(6,6)/6-31G* calculations; that was also the level employed to evaluate the spin−orbit couplings at these MECPs. For this purpose the method of Abegg[37] as implemented in the Gaussian98 suite of programs[38]

† Part of the special issue "Tomas Baer Festschrift".

10.1021/jp048253s CCC: $27.50
Published on Web 07/02/2004

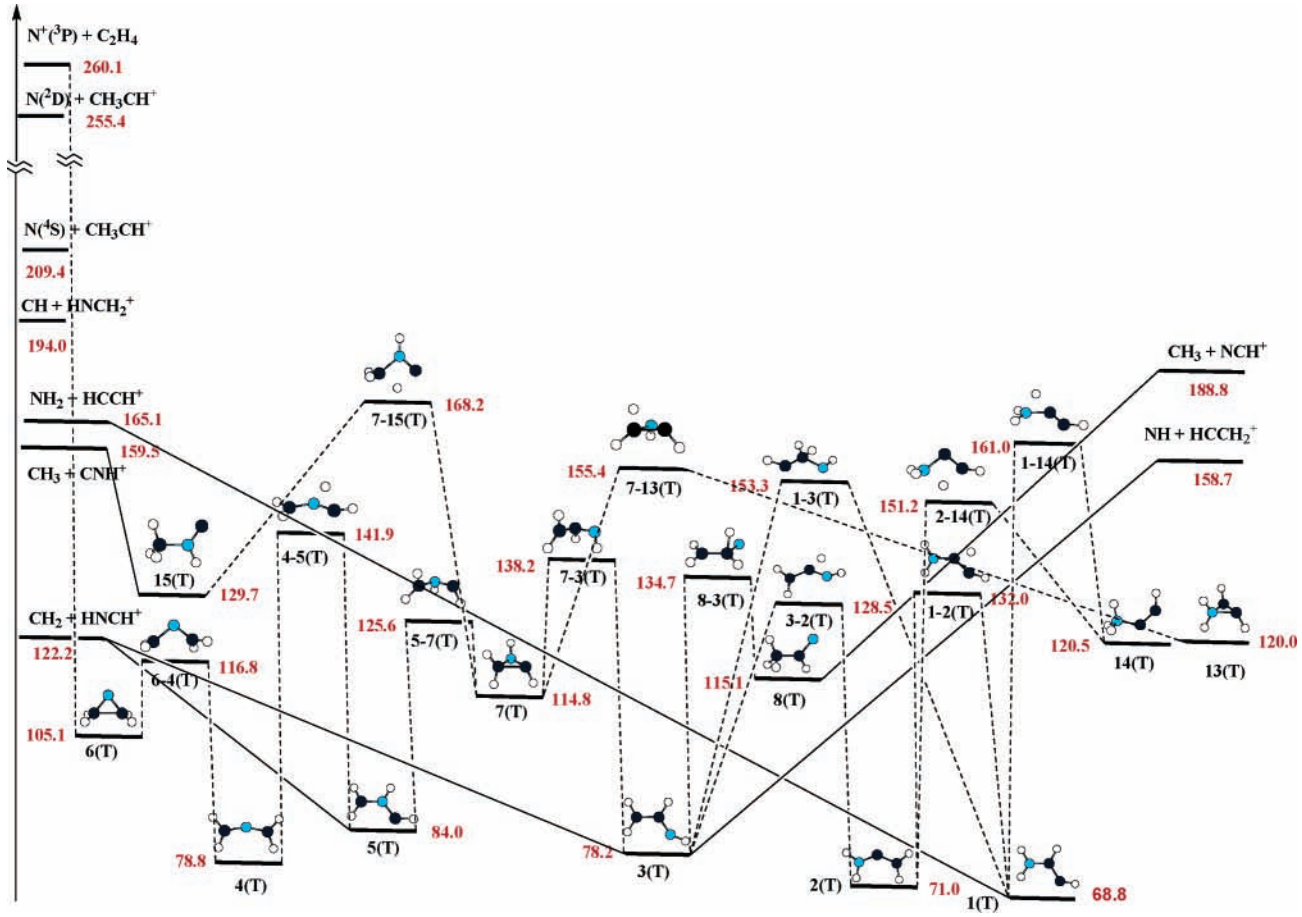

Figure 1. Potential energy surface associated with the $N^+(^3P) + C_2H_4$ reaction. Relative energies (in kcal mol^{-1}) are referred to the singlet global minimum **1(S)**. Solid lines connect the complexes with the appropriate dissociation limits.

was adopted. CASSCF(6,6)/6-31G* calculations were also used to locate the conical intersections associated with the dissociation of some molecular cations.

The bonding characteristics of the different singlet- and triplet-state cations were analyzed by means of the atoms-in-molecules (AIM) theory[39] and by means of the natural bond orbital (NBO) approach.[40] Using the first of these theoretical schemes, we have located the different bond critical points (bcp's) and their charge densities, which provide information on the relative strength of the bonds. A complementary picture is obtained through the use of the NBO method in terms of localized orbitals built up from atomic hybrids.

Results and Discussion

The PESs for the reaction $N^+(^3P) + C_2H_4$ has been schematized in Figure 1. That corresponding to the $N^+(^1D) + C_2H_4$ reaction is shown in Figure 2. The total energies and the geometries of the different stationary points and their zero point energies are given in Table 1S and Figure 1S of the Supporting Information. The different local minima are numbered following stability order and adding an "S" or a "T" within parentheses to distinguish singlet from triplet state cations. Hence, **1(T)** names the global minimum of the triplet potential energy surface, while **1(S)** designates the global minimum of the singlet potential energy surface. For the sake of a better comparison between both PESs, relative energies are referred to the singlet global minimum **1(S)**, which lies 68.8 kcal mol^{-1} below the triplet global minimum **1(T)**. It should be mentioned that the $N^+(^3P) + C_2H_4$ PES is similar to that reported by Di Stefano et al.[17] although, since our calculations have been carried out at the ab initio rather than the DFT level, there are some subtle differences as far as the relative stabilities of the different local minima and transitions states are concerned. It should also be mentioned that, for the sake of clarity, the PESs do not include all the local minima we have located, although they are included in the Supporting Information. For example, the $[CH_3-N-CH]^+$ **12(T)** isomer of structure **15(T)** ($[CH_3-NH-C]^+$) is not included in the energy profile, because the isomerization barrier between both forms is quite high. This applies also to the $[NH_3-CH-C]^+$ **11(T)** isomer of species $[NH_3-C-CH]^+$ **14(T)** and to the $[CH_3-C-NH]^+$ **9(T)** isomer of $[CH3-C(H)N]^+$ **8(T)**.

In general, the $[H_4, C_2, N]^+$ singlet-state cations are more stable than the corresponding triplet-state analogues, although the $N^+(^3P) + C_2H_4$ entrance channel lies 46.7 kcal mol^{-1} below the $N^+(^1D) + C_2H_4$ entrance channel. This clearly indicates that there are substantial bonding dissimilarities between singlets and triplets that render the former more stable than the latter, almost systematically.

Bonding Characteristics. Although a detailed analysis of the structures of the different cationic species involved in these reactions is not the aim of this paper, we still consider it useful to compare the geometries and bonding characteristics of singlet- and triplet-state cations that present similar connectivity. This is the case for the following couples that we are going to use as suitable examples: **3(S)** and **4(T)**, **4(S)** and **2(T)**, **8(S)** and **3(T)**, and **10(S)** and **5(T)** (see Figure 3).

A cursory examination of the structures of species **3(S)** and **4(T)** shows substantial differences between their optimized geometries. Whereas the triplet-state cation, **4(T)**, is planar, in the singlet both CH_2 groups lie in planes perpendicular to each

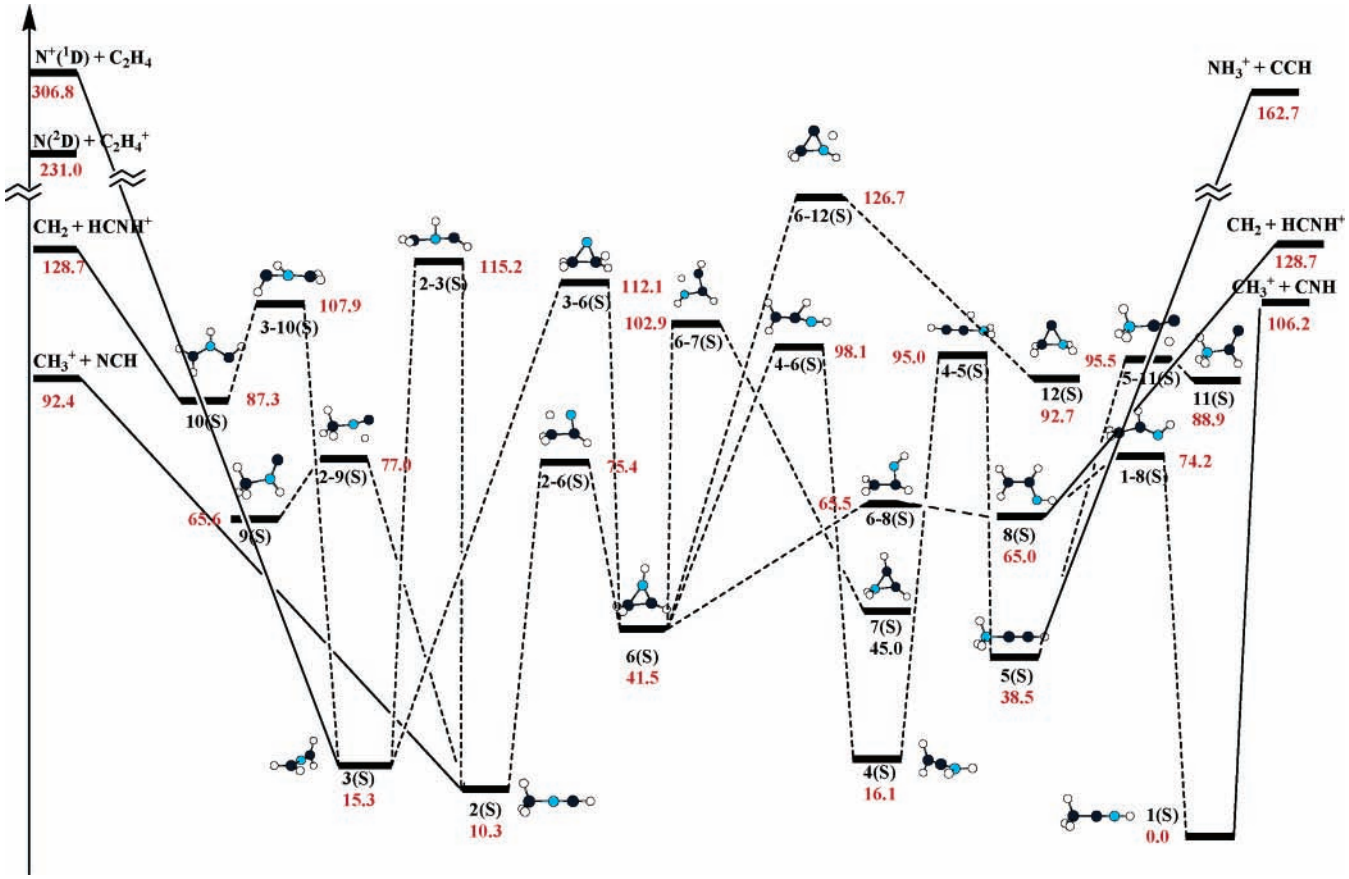

Figure 2. Potential energy surface associated with the $N^+(^1D) + C_2H_4$ reaction. All values in kcal mol^{-1}. Solid lines connect the complexes with the appropriate dissociation limits.

other. Also importantly, the charge density at the C−N bond critical point is larger in the singlet than in the corresponding triplet, and accordingly the bond length is shorter in the former. An NBO analysis of the bonding of these two species shows the existence of two C═N double bonds in the singlet, while in the triplet this possibility is forbidden because two electrons must have identical spin and therefore cannot be involved in the bonding. Accordingly, while in the singlet both methylene groups lie in perpendicular planes to favor the formation of the two C═N double bonds, in the triplet both lie in the same plane to favor a charge delocalization associated with the single occupancy of the C−N π-bonding orbital (see Figure 4). This charge delocalization is also reflected in the spin densities associated with the different atoms of the system as illustrated in Figure 4. Hence, it is not surprising to find that **3(S)** is predicted to be 63.5 kcal mol^{-1} more stable than **4(T)**. The aforementioned bonding differences are also mirrored in the corresponding stretching frequencies which in the triplet appear significantly red-shifted with respect to the singlet (see Table 1).

The situation is rather similar if one compares species **4(S)** and **2(T)**. Again the latter is planar, while in the former the NH_2 group is perpendicular to the plane that contains the methylene group. Once more in the singlet two double bonds (C═C and C═N) are formed, while in the triplet the C−C is a single bond, the two unpaired electrons being associated with both carbon atoms. Consistently, the C−C bond is much longer in the triplet (1.400 Å) than in the singlet (1.294 Å), whereas the charge density at the C−C bcp is larger in the latter. The C−N and C−C stretching frequencies appeared coupled as asymmetric and symmetric combinations, but again for the singlet they appear at higher frequency values than for the triplet (see Table 1).

The differences are much smaller when comparing **8(S)** and **3(T)** species. As a matter of fact, in the singlet-state cation the NBO localizes a C═N double bond and a single C−C bond. Conversely, for the triplet the C−C and the C−N σ-bonding orbitals are doubly occupied, but the π-bonding orbitals are singly occupied, the unpaired electrons being associated essentially to the methylene and the imino groups, respectively (see Figure 4). Consistently, the C−C bond length in the triplet is now slightly shorter and its stretching frequency slightly greater than in the singlet, while the opposite is true for the C−N bond, although in this case the charge densities at the bcp's do not follow the expected trend. The much smaller bonding differences are also reflected in a much smaller energy gap between both species, the triplet **3(T)** being only 13.3 kcal mol^{-1} less stable than **8(S)**. The situation is rather similar when one compares the minimum **10(S)** with the corresponding triplet **5(T)**. Again in the latter there is a C−N−C delocalization, while in the former the N−CH linkage is a single bond and the CH_2−N is double. The reinforcement of the N−CH linkage on going from the singlet to the triplet results in a significant shortening of the bond length, the triplet now being slightly more stable (3.3 kcal mol^{-1}) than the singlet.

Hence, in view of the substantial differences in bonding between singlet- and triplet-state cations it is not surprising to find that, despite the $N^+(^3P) + C_2H_4$ entrance channel being 46.7 kcal mol^{-1} below the $N^+(^1D) + C_2H_4$ entrance channel, the global minimum of the singlet PES lies 68.8 kcal mol^{-1} below the triplet global minimum.

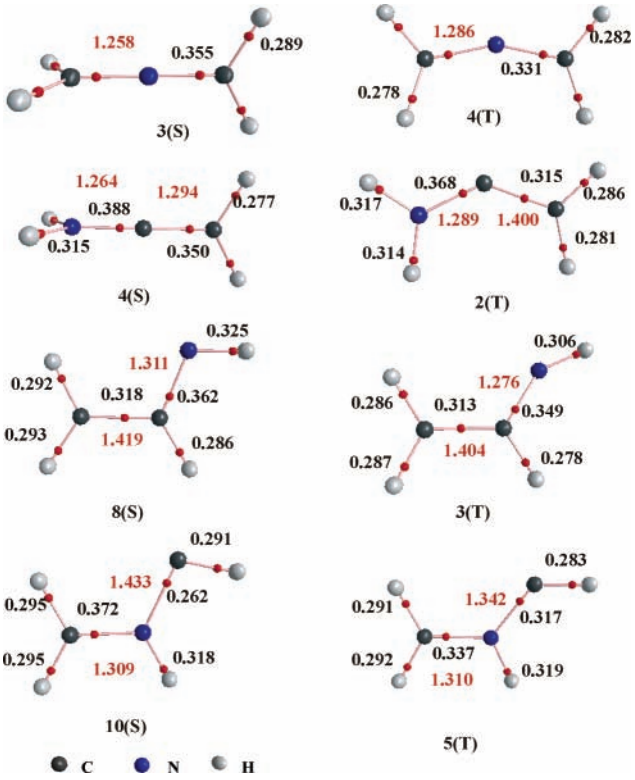

Figure 3. Molecular graphs of several singlet- and triplet-state $[H_4, C_2, N]^+$ cations with the same connectivity. Red points are bond critical points. Their charge densities are given in e au^{-3}. Bond lengths, in Å, are indicated in red.

TABLE 1: Stretching Frequencies (cm^{-1}) of Bonds Involving the Heavy Atoms of Some $[H_4, C_2, N]^+$ Singlet- and Triplet-State Cations

vibrational mode	3S	4T
CNC asym stretch	2103	1180
CNC sym stretch	1193	1120
vibrational mode	4S	2T
NCC asym stretch	2143	1735
NCC sym stretch	1145	1056
vibrational mode	8S	3T
CC stretch	1154	1259
C−N stretch	1621	1591
vibrational mode	10S	5T
$N-CH_2$ stretch	1689	1601
N−CH stretch	982	1059

$N^+(^3P) + C_2H_4$ Reaction Mechanisms. The direct interaction between ethylene and $N^+(^3P)$ yields a cyclic $[CH_2-N-CH_2]^+$ structure **6(T)** which is a conventional π-type complex (see Figure 1). From this structure the most favorable process is the opening of the ring, which actually corresponds to the insertion of the nitrogen atom into the C═C bond. This new structure $[CH_2-N-CH_2]^+$ **4(T)** would evolve through a 1,2-H shift toward complex $[CH-NH-CH_2]^+$ **5(T)**, which may dissociate into $CH + HNCH_2^+$ (125.2 kcal mol^{-1} above the global triplet minimum) or into $CH_2 + HCNH^+$, the former being much less favorable. Alternatively, **5(T)** may evolve through the transition state **5-7(T)** to yield a cyclic $[CH-NH-CH_2]^+$ intermediate **7(T)**. Although the activation barrier associated with the **5-7(T)** transition state is higher in energy than the $CH_2 + HCNH^+$ dissociation limit, it must be taken into account that very likely this dissociation also involves an activation barrier, since it necessarily implies a significant rearrangement of the electron distribution because, in the molecular cation, one of the two unpaired electrons as revealed by the corresponding spin densities is on the CH_2 terminal group and the other one is on the HCNH moiety, whereas in the products both unpaired electrons are on the CH_2 fragment. Therefore, a diabatic dissociation of **5(T)** would lead to some excited exit channel. In agreement with this expectation CASSCF(6,6)/6-31G* calculations show that **5(T)** complex has a relatively low lying excited state that would correlate diabatically with the dissociation limit $CH_2 + HCNH^+$. As a matter of fact, when the C−N bond is stretched in complex **5(T)**, the energy increases up to a conical intersection with this first excited state, which lies 111.3 kcal/mol above the triplet global minimum. Hence, we may conclude that the most favorable process with origin in species **5(T)** would be its isomerization to yield **7(T)**.

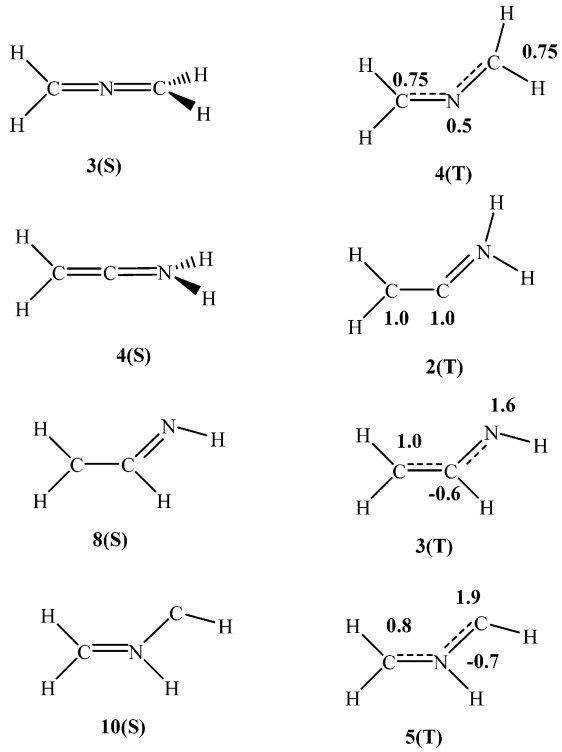

Figure 4. Bonding characteristics of several singlet- and triplet-state $[H_4, C_2, N]^+$ cations with the same connectivity. For the triplets the numbers correspond to the spin densities at the heavy atoms.

A bunch of possible reaction pathways have their origin in this cyclic structure through the transition states **7-15(T)**, **7-13(T)**, and **7-3(T)**. Species $[CH_3-N(H)C]^+$ **15(T)** formed in the first of these processes is a good precursor for the loss of CH_3, leaving CNH^+ as product ion, which is one of the ions experimentally detected in $N^+(^3P) + C_2H_4$ reactions.[33]

The most favorable of the three processes is, however, that leading to structure $[CH_2-CH-NH]^+$ **3(T)** which is the origin of another bunch of reaction pathways: (a) its dissociation into $CH_2 + HCNH^+$; (b) its dissociation into $NH + HCCH_2^+$; (c) its isomerization through the transition state **8-3(T)** to yield $[CH_3-C(H)N]^+$ **8(T)**; (d) its isomerization to yield the global minimum $[CH-CH-NH_2]^+$ **1(T)**; (e) its isomerization to yield the local minimum $[CH_2-C-NH_2]^+$ **2(T)**.

Both dissociation processes a and b lead to product ions that have been experimentally detected. However, while experimentally a higher proportion of $HCCH_2^+$ product ions formed in process b was found, our calculations predict dissociation a to be less endothermic than dissociation b. The situation is very

similar to that discussed above for **5(T)** species and for the same reasons, implying that the dissociation of $[CH_2-CH-NH]^+$ **3(T)** into $CH_2 + HCNH^+$ takes place through an activation barrier. The conical intersection associated with this process was found to be 63 kcal/mol above the triplet global minimum at the CASSCF(6,6)/6-31G* level of theory, rendering this dissociation kinetically less favorable than that leading to $NH + HCCH_2^+$.

Reaction pathway c would yield $[CH_3-C(H)N]^+$ **8(T)**, which is the precursor for the loss of methyl radical, which is one of the experimentally observed products. However, differently from complex $[CH_3-N(H)C]^+$ **15(T)** dissociation, the product ion is the less stable isomer HCN^+, and therefore it is likely that this dissociation would not occur. The same species could also dissociate, in principle, into $N(^4S) + CH_3-CH^+$, which lies 50.7 kcal mol^{-1} below the entrance channel, in a typical charge-transfer process. However, an inspection of the spin distribution of species $[CH_3-N(H)C]^+$ **15(T)** reveals that the spin density at the nitrogen atom is only 0.6 and therefore this complex would not dissociate into $N(^4S) + CH_3-CH^+$ but into $N(^2D) + CH_3-CH^+$, which lies 46 kcal mol^{-1} higher in energy. This is consistent with the fact that no charge transfer has been observed experimentally.

The fourth reaction pathway with origin in $[CH_2-CH-NH]^+$ **3(T)** leads, as mentioned above, to the global minimum of the triplet potential energy surface, which would eventually dissociate into $NH_2 + HCCH^+$, which are also experimentally observed products of the reaction.

The most favorable mechanism with origin in species $[CH_2-CH-NH]^+$ **3(T)** is, however, that leading to structure $[CH_2-C-NH_2]^+$ **2(T)**, which isomerizes to give the global minimum, which would eventually dissociate as mentioned above. Hence, the most favorable way to reach the global minimum of the PES is through species **2(T)** and not by a direct isomerization of **3(T)**.

$N^+(^1D) + C_2H_4$ Reaction Mechanisms. The interaction between $N^+(^1D)$ with ethylene leads to the direct insertion of the cation into the C═C bond as discussed before by Corral et al.[34] The molecular cation so formed, namely $[CH_2-N-CH_2]^+$ **3(S)**, may, in principle, dissociate into $CH_2^+ + NCH_2$, but the corresponding dissociation limit is very high in energy to compete with the possible isomerization processes leading to $[CH_3-N-CH]^+$ **2(S)**, cyclic $[CH_2-NH-CH]^+$ **6(S)**, and $[CH_2-NH-CH]^+$ **10(S)**. As shown in Figure 2, all of them involve rather similar activation barriers, the smallest one being that associated with the formation of species $[CH_2-NH-CH]^+$ **10(S)**, which would eventually dissociate into $CH_2 + HCNH^+$. The second possible isomerization process leads to species **6(S)**. Although a bunch of reaction pathways have their origin in this cyclic molecular cation, the most favorable one by far is that leading to $[CH_2-CH-NH]^+$ **8(S)**, which can be considered an intermediate to finally yield the global minimum of the potential energy surface, $[CH_3-C-NH]^+$ **1(S)**. The global minimum would dissociate into $CH_3^+ + CNH$. The formation of complex $[CH_3-N-CH]^+$ **2(S)** is the third possible isomerization process with origin in **3(S)**. This molecular cation would also yield CH_3^+ as ion product, but in this case the accompanying neutral is HCN and accordingly the corresponding dissociation limit lies 13.8 kcal mol^{-1} below that associated with the dissociation of the global minimum. It is worth noting that, alternatively, $[CH_3-N-CH]^+$ **2(S)** can isomerize to yield **6(S)** and $[CH_3-N(H)C]^+$ **9(S)**. The local minimum **9(S)** would yield upon dissociation the same products as the global minimum.

Hence, in principle only one of the expected products of the $N^+(^1D) + C_2H_4$ reaction, namely the $HCNH^+$ ion, coincides with those of the $N^+(^3P) + C_2H_4$ reaction. The most favorable processes in $N^+(^1D) + C_2H_4$ reactions are those producing CH_3^+, which is not formed in the $N^+(^3P) + C_2H_4$ reaction, and which, in turn, has not been observed experimentally.

TABLE 2: Spin−Orbit Couplings (SOC, cm^{-1}) at Several Minimum Energy Crossing Points between Singlet and Triplet $[H_4, C_2, N]^+$ Potential Energy Surfaces

species coupled	SOC	ΔE^a
2(T)−4(S)	1.4	0.6
3(T)−8(S)	23.4	9.2
4(T)−3(S)	16.0	41.5
5(T)−10(S)	13.9	16.7
14(T)−5(S)	8.8	45.1

[a] ΔE (kcal mol^{-1}) corresponds to the energy barrier from the corresponding triplet minimum.

Intersystem Crossing. The fact that many of the local minima of the singlet potential energy surface lie lower in energy than the corresponding triplets, even though the triplet entrance channel is lower in energy than the singlet one, clearly indicates that both hypersurfaces must cross each other. No doubt, in view of the topology of both PESs, several minimum energy crossing points may exist. To locate the most significant ones, we have chosen triplet- and singlet-state cations with similar connectivity. A summary of the results obtained is given in Table 2.

It can be seen that the most efficient of these couplings is that connecting the **3(T)** triplet-state cation with the **8(S)** singlet, which is also associated with a small energy barrier. Also, the **5(T)−10(S)** coupling can be quite efficient, while in the other cases either the energy gap is quite large or the spin−orbit coupling is quite small.

Hence, in principle a triplet−singlet crossover in $N^+ + C_2H_4$ reactions cannot be discarded. This implies the possibility of reaching structures **8(S)** and **10(S)** through spin-forbidden processes, and therefore the possibility of forming the singlet global minimum and its eventual dissociation into $CH_3^+ + CNH$.

Therefore, why CH_3^+ was not observed in $N^+(^3P) + C_2H_4$ reactions is an open question that requires a dynamic treatment beyond the scope of this paper.

Conclusions

Singlet- and triplet-state $[H_4, C_2, N]^+$ cations exhibit very different bonding patterns. In general, the level of unsaturation in singlet-state ions is larger than that in their triplet counterparts, and accordingly, the singlets are almost systematically more stable than the triplets. As a matter of fact, even though the $N^+(^3P) + C_2H_4$ entrance channel lies 46.7 kcal mol^{-1} below the $N^+(^1D) + C_2H_4$, the global minimum of the singlet PES lies 68.8 kcal mol^{-1} below the global minimum of the triplet PES.

This makes possible a crossover between both PESs that may lead to spin-forbidden mechanisms. Several minimum energy crossing points between both hypersurfaces have been located, and the corresponding spin−orbit couplings indicate that indeed spin-forbidden processes in $N^+ + C_2H_4$ reactions cannot be discarded. According to our survey, the product distribution in both $N^+(^3P) + C_2H_4$ and $N^+(^1D) + C_2H_4$ reactions should be quite different. While for the triplets the CNH^+, $HCNH^+$, $HCCH_2^+$, and $HCCH^+$ product ions should be observed, in agreement with the available experimental information, for the singlets the formation of CH_3^+ should be the dominant process.

Acknowledgment. This work has been partially supported by DGI Project No. BQU2003-00894. I.C. gratefully acknowl-

edges an FPU grant from the Ministerio de Educación, Cultura y Deporte of Spain. A generous allocation of computational time at the CCC of the UAM and at the Computational Center of CIEMAT is gratefully acknowledged.

Supporting Information Available: Calculated G2(MP2) total energies and MP2/6-31G* optimized geometries of the stationary points on the $N^+(^3P) + C_2H_4$ and $N^+(^1D) + C_2H_4$ potential energy surfaces. This material is available free of charge via the Internet at http://pubs.acs.org.

References and Notes

(1) Anicich, V. G. J. *J. Phys. Chem. Ref. Data* **1993**, *22*, 1469−1569.
(2) Largo, A.; Flores, J. R.; Barrientos, C.; Ugalde, J. M. *J. Phys. Chem.* **1991**, *95*, 170−175.
(3) Largo, A.; Redondo, P.; Barrientos, C.; Ugalde, J. M. *J. Phys. Chem.* **1991**, *95*, 3−5445.
(4) Largo, A.; Flores, J. R.; Barrientos, C.; Ugalde, J. M. *J. Phys. Chem.* **1991**, *95*, 6553−6557.
(5) López, X.; Ugalde, J. M.; Barrientos, C.; Largo, A.; Redondo, P. *J. Phys. Chem.* **1993**, *97*, 1521−1527.
(6) Esseffar, M.; Luna, A.; Mó, O.; Yáñez, M. *J. Phys. Chem.* **1994**, *98*, 8679−8686.
(7) Largo, A.; Barrientos, C.; López, X.; Ugalde, J. M. *J. Phys. Chem.* **1994**, *98*, 3985−3991.
(8) Luna, A.; Manuel, M.; Mó, O.; Yáñez, M. *J. Phys. Chem.* **1994**, *98*, 6980−6987.
(9) McCarthy, M. C.; Travers, M. J.; Kovacs, A.; Chen, W.; Novick, S. E.; Gottlieb, C. A.; Thaddeus, P. *Science* **1997**, *275*, 518−520.
(10) González, A. I.; Mó, O.; Yáñez, M. *Int. J. Mass Spectrom.* **1998**, *179*, 77−90.
(11) Flores, J. R.; Estevez, C. M. *J. Phys. Chem. A* **2000**, *104*, 11095−11105.
(12) Millar, T. J.; Flores, J. R.; Markwick, A. J. *Mon. Not. R. Astron. Soc.* **2001**, *327*, 1173−1177.
(13) Ijjaali, F.; El-Mouhtadi, M.; Esseffar, M.; Alcamí, M.; Mó, O.; Yáñez, M. *Phys. Chem. Chem. Phys.* **2001**, *3*, 179−183.
(14) Flores, J. R.; Estevez, C. M.; Carballeira, L.; Pérez Juste, I. *J. Phys. Chem. A* **2001**, *105*, 4716−4725.
(15) Flores, J. R.; Pérez Juste, I.; Carballeira, L.; Estevez, C. M.; Gómez, F. *Chem. Phys. Lett.* **2001**, *342*, 105−112.
(16) Flores, J. R.; Gómez, F. *J. Phys. Chem. A* **2003**, *107*, 914−935.
(17) Di Stefano, M.; Rosi, M.; Sgamellotti, A. *Chem. Phys.* **2004**, *297*, 121−131.
(18) Chen, W.; Novick, S. E.; McCarthy, M. C.; Thaddeus, P. *J. Chem. Phys.* **1998**, *109*, 10190−10194.
(19) Apponi, A. J.; McCarthy, M. C.; Gottlieb, C. A.; Thaddeus, P. *J. Chem. Phys.* **1999**, *111*, 3911−3918.
(20) Apponi, A. J.; McCarthy, M. C.; Gottlieb, C. A.; Thaddeus, P. *Astrophys. Lett.* **1999**, *516*, L103−L104.
(21) Bell, M.; Feldmann, P. A.; Travers, M. J.; McCarthy, M. C.; Gottlieb, C. A.; Thaddeus, P. *Astrophys. J.* **1997**, *483*, L61.
(22) Wiese, W. L.; Smith, M. W.; Glennon, B. M. *Atomic Transition Probabilities*; NSRDS-NBS 4; U.S. Government Printing Office: Washington DC, 1966; Vol. 1.
(23) Manuel, M.; Mó, O.; Yáñez, M. *Mol. Phys.* **1997**, *91*, 503−512.
(24) Manuel, M.; Mó, O.; Yáñez, M. *J. Phys. Chem. A* **1997**, *101*, 1722−1730.
(25) Manuel, M.; Mó, O.; Yáñez, M. *Mol. Phys.* **1999**, *96*, 231−241.
(26) Fernández-Morata, F.; Alcamí, M.; González, L.; Yáñez, M. *J. Phys. Chem. A* **2000**, *104*, 8075−8080.
(27) Ijjaali, F.; Alcamí, M.; Mó, O.; Yáñez, M. *J. Phys. Chem. A* **2000**, *104*, 11132−11139.
(28) Ijjaali, F.; Alcamí, M.; Mó, O.; Yáñez, M. *Int. J. Quantum Chem.* **2002**, *86*, 130.
(29) Anicich, V. G. J.; McEwan, M. J. *Planet. Space Sci.* **1997**, *45*, 897.
(30) Salama, F.; Galazutdinov, G. A.; Krelowski, J.; Allamandola, L. J.; Musaev, F. A. *Astrophys. J.* **1999**, *526*, 265.
(31) Smith, D. *Chem. Rev.* **1992**, *92*, 1473.
(32) Ascenzi, D.; Franceschi, P.; Freegarde, T. G. M.; Tosi, P.; Bassi, D. *Chem. Phys. Lett.* **2001**, *356*, 35.
(33) Smith, D.; Adams, N. G. *Chem. Phys. Lett.* **1980**, *76*, 418.
(34) Corral, I.; Mó, O.; Yáñez, M. *Int. J. Quantum Chem.* **2003**, *91*, 438.
(35) Scott, A. P.; Radom, L. *J. Phys. Chem.* **1996**, *100*, 16502−16513.
(36) Curtiss, L. A.; Raghavachari, K.; Pople, J. A. *J. Chem. Phys.* **1993**, *98*, 1293−1298.
(37) Abegg, P. W. *Mol. Phys.* **1975**, *30*, 579.
(38) Frisch, M. J.; Trucks, G. W.; Schlegel, H. B.; Scuseria, G. E.; Robb, M. A.; Cheeseman, J. R.; Zakrzewski, V. G.; Montgomery, J. A.; Stratmann, R. E.; Burant, J. C.; Dapprich, S.; Millam, J. M.; Daniels, A. D.; Kudin, K. N.; Strain, M. C.; Farkas, O.; Tomasi, J.; Barone, V.; Cossi, M.; Cammi, R.; Mennucci, B.; Pomelli, C.; Adamo, C.; Clifford, S.; Ochterski, J.; Petersson, G. A.; Ayala, P. Y.; Cui, Q.; Morokuma, K.; Malick, D. K.; Rabuck, A. D.; Raghavachari, K.; Foresman, J. B.; Cioslowski, J.; Ortiz, J. V.; Stefanov, B. B.; Liu, G.; Liashenko, A.; Piskorz, P.; Komaromi, I.; Gomperts, R.; Martin, R. L.; Fox, D. J.; Keith, T.; Al-Laham, M. A.; Peng, C. Y.; Nanayakkara, A.; González, C.; Challacombe, M.; Gill, P. M. W.; Johnson, B.; Chen, W.; Wong, M. W.; Andres, J. L.; González, C.; Head-Gordon, M.; Replogle, E. S.; Pople, J. A. In *Gaussian98*, revised A3 ed.; Gaussian, Inc.: Pittsburgh, PA, 1999.
(39) Bader, R. F. W. *Atoms In Molecules: A Quantum Theory*; Clarendon Press Oxford University: Oxford, 1990.
(40) Reed, A. E.; Curtiss, L. A.; Weinhold, F. *Chem. Rev.* **1988**, *88*, 899.